LBL--27610

DE90 000172

Pion and Kaon Interferometry of Nuclear Collisions*

Miklos Gyulassy and Sandra S. Padula[1]

Nuclear Science Division
Mailstop 70A-3307
Lawrence Berkeley Lab
Berkeley, CA 94720 USA

August 4, 1989

Abstract:
In the study complex reactions, the simple space-time interpretation of pion interferometry often breaks down due to strong correlations between spatial and momentum coordinates. In those cases, pion interferometry is still useful as a complementary test of specific dynamic models, but a refined formalism must be used, as discussed in the introduction. With this formalism, we show that recent NA35 data on $O + Au \to \pi^-\pi^- + X$ at 200 AGeV are consistent with both hadronic resonance and quark-gluon plasma models for this reaction. The sensitivity of the outward and sideward transverse projected correlation function for pions is investigated. Finally, we compare pion and kaon interferometry predictions of these two models.

To appear in Proc. International Advanced Courses on "THE NUCLEAR EQUATION OF STATE", Peniscola, Spain, May 21 - June 3, Plenum Publishing Co. Ltd. (London).

[0]*This work was supported by the Director, Office of Energy Research, Division of Nuclear Physics of the Office of High Energy and Nuclear Physics of the U.S. Department of Energy under Contract No. DE-AC03-76SF00098.

[0]1. Supported by Conselho Nacional de Desenvolvimento Científico e Tecnológico (CNPq), Brazil

PION AND KAON INTERFEROMETRY OF NUCLEAR COLLISIONS[†]

Sandra S. PADULA[*] and Miklos GYULASSY

Mailstop 70A-3307, Lawrence Berkeley Laboratory, Berkeley, CA 94720 USA

In the study complex reactions, the simple space-time interpretation of pion interferometry often breaks down due to strong correlations between spatial and momentum coordinates. In those cases, pion interferometry is still useful as a complementary test of specific dynamic models, but a refined formalism must be used, as discussed in the introduction. With this formalism, we show that recent NA35 data on $O + Au \to \pi^-\pi^- + X$ at 200 AGeV are consistent with both hadronic resonance and quark-gluon plasma models for this reaction. The sensitivity of the outward and sideward transverse projected correlation function for pions is investigated. Finally, we compare pion and kaon interferometry predictions of these two models.

1 Introduction

Pion interferometry has been used for a long time[1]-[19] to probe the space-time geometry of high energy hadronic reactions (for a comprehensive review, see [20]). It is based on exploiting the constructive interference between identical bosons when their relative momenta are small compared to the inverse of the typical spatial dimensions of the reaction volume. Experimentally, the interference pattern is deduced by measuring like pion correlation functions,

$$C_n(\mathbf{k}_1, \cdots, \mathbf{k}_n) = \mathcal{N}_n P_n(\mathbf{k}_1, \cdots, \mathbf{k}_n) / \prod_{i=1}^{n} P_1(\mathbf{k}_i) \ , \tag{1}$$

where P_n denotes the n (identical) pion inclusive distributions, and $\mathcal{N}_n$ is the inverse of the normalized n^{th} factorial moment of the multiplicity distribution.

Unfortunately, the simple geometrical interpretation of the interference pattern is only valid in the semi-classical limit and in the absence of correlations between the spatial and momentum coordinates[6, 7]. In such idealized cases, the two pion correlation function $C_2(\mathbf{k}_1, \mathbf{k}_2)$ is directly related to the space-time density, $\rho(x)$, of pion emission points through

$$C_2(\mathbf{k}_1, \mathbf{k}_2) \equiv P_2(k_1, k_2)/P_1(k_1)P_1(k_2) = 1 + \lambda |\rho(k_1 - k_2)|^2 \ , \tag{2}$$

[0]†This work was supported by the Director, Office of Energy Research, Division of Nuclear Physics of the Office of High Energy and Nuclear Physics of the U.S. Department of Energy under Contract No. DE-AC03-76SF00098.

[0]* Supported by Conselho Nacional de Desenvolvimento Científico e Tecnológico (CNPq), Brazil

with $\rho(q) = \int d^4x e^{iq\cdot x}\rho(x)$ and with the incoherence or chaoticity parameter $\lambda = 1$. In many interesting cases, dynamical effects can lead, however, to strong correlations between $\mathbf{x}$ and $\mathbf{k}$ which can distort the interference pattern and obscure the space-time interpretation of $C(\mathbf{k}_1, \mathbf{k}_2)$. In such cases the analysis of correlation functions necessarily becomes model dependent! Nevertheless, the study of small relative momentum pion correlations is still useful as a unique and complementary test of specific dynamical models since identical pion correlations are sensitive to the *phase space correlations* predicted by transport models, which are otherwise not tested in other inclusive measurements. However, as shown in Ref[21] it is essential in that case to use a more refined formalism to connect transport calculations with interferometry data.

A characteristic symptom of the breakdown of the ideal picture is that $C_2(\mathbf{k}_1, \mathbf{k}_2)$ is found to depend on the mean pion momentum, $\mathbf{K} = (\mathbf{k}_1 + \mathbf{k}_2)/2$, as well as on the relative momentum, $\mathbf{q} = \mathbf{k}_1 - \mathbf{k}_2$ even in the case $\mathbf{K} \cdot \mathbf{q} = 0$ (see e.g. [7, 8, 10, 14]). (A dependence on the component of $\mathbf{K}$ parallel to $\mathbf{q}$ always occurs if there is time dependence of $\rho(\mathbf{x}, t)$.) A second symptom of the breakdown of the ideal picture is a fitted value of $\lambda < 1$, also found often experimentally. While in principle partially coherent fields could be produced[5], the most likely cause of an apparent $\lambda < 1$ is an overly simplified analysis of the complex six-dimensional dependence of $C_2(\mathbf{k}_1, \mathbf{k}_2)$ involving integrations over four or five of the momentum variables and/or neglecting additional important dynamical degrees of freedom such as resonances. These points have been emphasized for example in refs.[14, 19].

Present interest in this problem stems from new data on pion interferometry of nuclear collisions at CERN[15] and the development of Monte Carlo transport models[18, 22] for high energy reactions. At high energies, Lorentz boost invariance along the beam direction leads to a strong (so called Inside-Outside[23]) correlation between the production points, x^μ, and final momenta, p^μ. The modifications of C_2 due to such phase space correlations have been studied in Refs.[11, 12, 14, 17] using a variety of simplifying assumptions and techniques. There has also been recent progress toward more realistic calculations, taking into account additional dynamical complications predicted by detailed transport models in refs.[18, 19]. However, the theoretical basis for those calculations has not been adequately discussed in the literature.

The formula derived in Ref.[21] turns out to be a natural generalization of the one proposed by Pratt[7] and is derived in a more comprehensive way using transport theory and the Wigner density formalism developed by Remler[24, 25]. Finite wavepackets are used to expose the sensitivity of the interference effects to the production mechanism.

The Wigner formalism connects the *rate of change* of the n particle phase space distribution, $f_n(\mathbf{x}_1, \mathbf{p}_1, \cdots, \mathbf{x}_n, \mathbf{p}_n, t)$ to asymptotic observables. As emphasized in [24, 25], transport theories, such as hydrodynamics or cascade models, can only approximate the rate of change of f_n during the limited time interval when relatively high momentum transfer processes are occuring. At asymptotic times such models break down or predict free streaming. Low momentum transfer final state interactions leading to weakly bound states[25] and subtle Bose interference effects can only be

rigorously extracted from transport models using the Wigner formalism. The formalism also allows us to derive a new equation incorporating effects of intermediate time cascading of pions and to study the conditions under which only the final freeze-out coordinates dominate the interference pattern.

The main result of Ref.[21] is summarized by the following formula for the Bose-Einstein symmetrized n pion invariant distribution:

$$P_n(\mathbf{k}_1,\cdots,\mathbf{k}_n) \propto \left\langle \sum_{\sigma} \prod_{j=1}^{n} e^{i(k_j-k_{\sigma_j})\cdot x_j} \delta_\Delta(k_j,k_{\sigma_j},p_j) \right\rangle \quad , \tag{3}$$

with the smoothed delta function given by

$$\delta_\Delta(k,k',p) = (2\pi\Delta p^2)^{-3/2}\exp(\tfrac{1}{2}(p-\tfrac{1}{2}(k+k'))^2/\Delta p^2 + \tfrac{1}{2}(k-k')^2\Delta x^2) \quad . \tag{4}$$

The brackets $\langle\cdots\rangle$ denote an average over the $8n$ pion *freeze-out* space coordinates $\{x_1,p_1,\cdots,x_n,p_n\}$, as obtained from the output of a specific transport model such as a cascade[18] or LUND model[19]. In this form, Eq.(4) is ideally suited for Monte Carlo computation of pion interference effects. The smoothed delta function results from the use of Gaussian wavepackets with widths Δx and Δp that depend on details of the pion production mechanism. The sum is over $n!$ permutations, $\sigma = (\sigma_1,\cdots,\sigma_n)$, of the indices ($x,k,p,\cdots$ denote four vectors and all momenta are on-shell).

There are several important points to note in connection with (3):

1. The freeze-out coordinates do not correspond in general to the set of coordinates $\{\mathbf{x}_i(t_f),\mathbf{p}_i(t_f)\}$ at any particular "freeze-out" time since the decoupling times, x_i^0, are usually widely distributed[24, 25]. In a cascade model, the freeze-out time for particle i is the time, t_{fi}, when the last binary collision was suffered by that particle and $(x_i^\mu,p_i^\mu) = (x^\mu(t_{fi}),p^\mu(t_{fi}+\epsilon))$. These $8n$ coordinates can be arbitrarily correlated.

2. The wavepacket widths enters because the uncertainty principle permits us to interpret the (x_i^μ,p_i^μ) only as the mean values of the pion wavepackets. In Monte Carlo calculations involving a finite sample of freeze-out coordinates, the interference terms are nonvanishing only if $\Delta p > 0$ since no two p_i are ever the same. However, in the semi-classical limit ($\langle(\mathbf{x}_i-\mathbf{x}_j)^2\rangle \gg \Delta x^2$, $\langle(\mathbf{p}_i-\mathbf{p}_j)^2\rangle \gg \Delta p^2$), the dependence on the widths drops out.

3. Eq.(3) reduces to the expression derived via a covariant current ensemble formalisms[19] for minimal wavepackets ($\Delta x\Delta p = \frac{1}{2}$). In that case $\Delta p^2 = mT$ in terms of the pion mass and the pseudo-temperature parameter characterizing current elements. Our derivation thus clarifies the interpretation of the current elements in the later formalism.

4. The Pratt[7] formula for interferometry correspond to the nonrelativistic and the $\Delta x = \Delta p = 0$ limits of (3). The hybrid Yano-Koonin formula[4] follows from (3) only if correlations between x_i and p_i can be neglected. In addition the wavepackets provide a physical basis for the numerical smoothing proceedure adopted in [18].

5. In general, correction terms to (3) appear due to cascading prior to the freeze-out time but can be neglected in the limit that the mean free path of pions is small compared to the source size (the hydrodynamic limit) or if the momentum transfers are small compared to the pion momenta (the Eikonal limit).

6. In cases where P_n is found to be sensitive to the wavepacket size, pion interferometry cannot separate production dynamics from the transport dynamics, and Δx and Δp must be treated as addition physical parameters. A similar sensitivity to the form of the current elements in the current ensemble method is possible. As we emphasize in Ref[21], this is the case for the ideal Inside-Outside cascade dynamics[11]-[19], where the rapidity correlation scale, $\delta y \sim (\tau \Delta p)^{-1}$, depends not only on the mean pion freez-out proper time but also on Δp.

7. Eq.(3) could be further generalized by allowing every packet to vary independently, e.g., via a different $\Delta x_i, \Delta p_i$. Choosing, the coherence length Δx_i to be very large for a fraction of the pions due to some exotic production mechanism, the interference pattern would be similar to that due to partially coherent fields[5].

8. Relative Coulomb and other final state interactions are not considered here but can be included via methods dicussed by Bowler[16].

2 Pion Interferometry of O + Au

The NA35 collaboration[15] measured $\pi^-\pi^-$ correlations in O+Au at 200 AGeV and reported that the freeze-out distribution for pions in this reaction is characterized by a surprisingly large freeze-out proper time and transverse radius, $\tau_f \sim R_{\perp f} \sim 7$ fm. In addition, they reported an unusually high degree of coherence for pions away from the central rapidity region. These results are of interest because they may imply a breakdown of popular hadronic transport models like LUND[22, 26] and possibly provide evidence for novel dynamical effects associated with the formation of quark-gluon plasma in nuclear collisions[11, 18].

In Ref.[19] we showed, however, that the above results are not conclusive and that the present data are in fact consistent with a wide range of pion source parameters when additional non-ideal dynamical and geometrical degrees of freedom are incorporated into the analysis. In particular, both hadronic transport models[22] and quark-gluon plasma hydrodynamic models[18] are found to be consistent with the present correlation data. We also study the sensitivity of "outward" and "sideward" transverse momentum interferometry[11, 18] and show that, in contrast to first expectations, much higher precision data will be required to differentiate between such competing dynamical models.

In its simplest form, pion interferometry involves fitting the $\pi\pi$ correlation function with the ansatz given by eq.(2). As discussed in the Introduction, this simple relation is, however, only valid if the freeze-out space-time and momentum coordinates of the pions are uncorrelated. In high energy hadronic processes there are many potential

sources of such correlations which can significantly modify[11, 12, 14, 17] the form of $C(k_1, k_2)$, and thus, the geometrical parameters obtained with (2) could be misleading. In phase-space, strong correlations[23] between the space-time and momentum rapidity variables, defined by $\eta = \frac{1}{2}\log((t+z)/(t-z))$ and $y = \frac{1}{2}\log((E+p_z)/(E-p_z))$, resulting from approximate longitudinal boost invariance, have to be taken into account. In addition, a large fraction of the observed π^- could arise from the decay of long lived resonances such as $\omega, K^*, \eta, \cdots$ [28]. It has been known for a long time[29] that those resonances can produce effects that could be misinterpreted as due to unusually long lived sources and partially coherent fields. For nuclear collisions at moderate energies $\sim$200 AGeV, additional complications due to non-uniformity of the rapidity density[15] and the large spread of pion freeze-out proper times must also be considered. Other correlations, e.g., between the transverse coordinate ($\mathbf{x}_\perp$) and the transverse momentum component ($\mathbf{p}_\perp$), may have to be considered if collective hydrodynamic flow occurs[11].

To incorporate these many effects into the pion interferometric analysis of nuclear collisions, we must use equations (3) and (4). While those equations were derived using the Wigner formalism, we now review the simpler current ensemble method that leads to the same equation for the case of minimal packets. In that formalism the source of pions is represented by a large ensemble of current elements, $\{j_a(x) = j_0(u_a^\mu(x - x_a)_\mu)\}$, where x_a^μ and u_a^μ denote the space-time origin and four-velocity of current element a, and $j_0(x)$ specifies each current element in its rest frame. The amplitude for the production of a pion with momentum k is given by the Fourier transform of the total source current,

$$j(k) = \sum_a j_0(u_a k) e^{ikx_a} e^{i\phi_a} \quad , \tag{5}$$

where the factors $e^{i\phi_a}$ are random phases in the case of completely chaotic sources. The m-pion inclusive distribution function is then given by

$$P_m(k_1, \cdots, k_m) = \langle \mid j(k_1) \mid^2 \cdots \mid j(k_m) \mid^2 \rangle \quad , \tag{6}$$

where $\langle \cdots \rangle$ denotes the ensemble average over the space-time coordinates x_a, four-velocities u_a, and random phases ϕ_a. In the absence of dynamical multi-pion correlations, that ensemble average can be expressed in terms of a "freeze-out" phase-space distribution

$$D(x, p) = \langle \delta^4(x - x_a)\delta^4(p - p_a) \rangle \quad , \tag{7}$$

where $p_a^\mu = m u_a^\mu$. The m pion inclusive distribution functions is then given by[5, 12]

$$P_m(k_1, \cdots, k_m) = \sum_\sigma \left\{ \prod_{i=1}^m G(k_i, k_{\sigma_i}) \right\} \quad , \tag{8}$$

where $\sigma = (\sigma_1, \cdots, \sigma_m)$ runs over the $m!$ permutations of indices. The complex amplitude $G(k_i, k_j)$ is given by the convolution of the freeze-out distribution and two current elements that characterize the production dynamics,

$$G(k_i, k_j) = \int d^4p D(k_i - k_j, p) j_0^*(pk_i/m) j_0(pk_j/m) = \langle e^{i(k_i - k_j)x_a} j_0^*(p_a k_i/m) j_0(p_a k_j/m) \rangle \quad . \tag{9}$$

The objective of pion interferometry from this point of view is to constrain the form of the freeze-out source distribution. The model dependence enters, however, not only through the parameterization of $D(x,p)$ but also through the model adopted for $j_0(k)$. In this formalism the current elements play the same role as wavepackets do in the Wigner density formalism[11, 21]. From (9) it is clear that (2) can apply only in the very special case that $D(q,p) \approx \rho(q)f(p)$, and that $f(p)$ is sharply peaked compared to $j_0(k)$. In other words, the space-time and velocity coordinates of the source elements must be uncorrelated and the Doppler shift of the pion spectra from each source element must be negligible. Neither of these conditions is satisfied in high energy hadronic processes.

In our calculations, we adopt for simplicity a covariant pseudo-thermal model for the current elements[5, 12],

$$j_0(pk/m) = \exp(-pk/(2mT)) \ . \tag{10}$$

where the effective "temperature", T, characterizes the spread of the source elements in momentum space and controls the transverse momentum distribution of pions in our case. With this model the amplitude assumes the particularly simple form

$$G(k_1,k_2) = \langle \exp\{iqx_a - Kp_a/(mT)\}\rangle \ , \tag{11}$$

depending not only on $q^\mu = k_1^\mu - k_2^\mu$ but also on the mean pair momentum $K^\mu = \frac{1}{2}(k_1^\mu + k_2^\mu)$. Note that this dependence is, however, quite different from the K dependence arising in the non-covariant Wigner formalism[11, 21].

The effects of long lived resonances can be easily included in the semiclassical approximation. Note that the pion freeze-out coordinates, x_a^μ, are related to its parent resonance production coordinates, x_r^μ, through

$$x_a^\mu = x_r^\mu + u_r^\mu \tau \ , \tag{12}$$

where u_r^μ is the resonance four velocity and τ is the proper time of its decay. Inserting (12) into (11), summing over resonances r of widths Γ_r, and averaging over their decay proper times, we obtain the final expression

$$G(k_1,k_2) \approx \langle \sum_r f_r \,(1 - iqu_r/\Gamma_r)^{-1} \exp(iqx_r - Ku_r/T_r)\rangle \ , \tag{13}$$

where f_r is the fraction of the observed π^-'s arising from the decay of a resonance of type r, and T_r characterizes the decay distribution of that resonance. The factor $(1 - iqu_r/\Gamma_r)^{-1}$ insures that pions arising from decay of long lived resonances do not interfere effectively at moderate q. While (13) is only valid in the semiclassical limit and involves an idealized model (10) of the decay dynamics, it is manifestly Lorentz covariant and is of sufficient generality to allow the study a variety of nontrivial dynamical models of high energy nuclear collisions.

We consider here a class of dynamical models that can be characterized by a set of resonance fractions $\{f_r\}$, and a freeze-out phase space distribution of the form

$$D(x,p) \propto \tau e^{-\tau^2/\tau_f^2} e^{-(\eta-y)^2/2\Delta\eta^2} e^{-(y-y^*)^2/2Y_c^2} e^{-r_\perp^2/R_\perp^2} \ , \tag{14}$$

where τ_f specifies the width and mean value of the freeze-out proper time, $\tau = (t^2 - z^2)^{1/2}$, distribution, $\Delta\eta$ specifies the rms fluctuations of $\eta = \frac{1}{2}\log((t+z)/(t-z))$ around $y = \frac{1}{2}\log((E+p_z)/(E-p_z))$, Y_c is the width of the rapidity distribution centered at y^*, and $R_\perp$ is the rms transverse radius at freeze-out. In this work, we estimate the parameters of the freeze-out distribution and resonance fractions using the ATTILA version of the LUND Fritiof multi-string model[22] and a string tension, $\kappa = 1$ GeV/fm, to map momentum space into coordinate space. For O+Au at 200 AGeV, we find that $Y_c \approx 1.4$, $y^* = 2.5$, $\Delta\eta \approx 0.7$, $\tau_f \approx 3$ fm/c and $R_\perp \approx 3$ fm. The π^- pedigree is determined to be $f_\pi = 0.19$, $f_\rho = 0.40$, $f_\omega = 0.16$, and $f_{K^*} = 0.09$, in rough agreement with data on hadron-hadron reactions[28]. The contribution from longer lived resonances is set to zero.

In Ref.[18] a similar form for D was employed to parametrize the results of a quark-gluon plasma hydrodynamic calculation. In that case, the parameters were found to be $\tau_f = 9.0$ fm/c,$R_\perp = 3.3$ fm,$\Delta\eta = 0.76$, assuming that $Y_c = \infty$ and neglecting resonances. The characteristic long lifetime found in such hydrodynamic models results from the slowness of the hadronization transition[30, 14, 17] when the latent heat of transition is large.

For comparison, the idealized inside-outside cascade model[23] considered in [5, 12] and used in [15] to fit the data corresponds to

$$D(x,p) \propto \delta(\tau - \tau_f)\delta(\eta - y)\exp(-r_\perp^2/R_\perp^2) \ , \tag{15}$$

with resonances neglected.

Given the freeze-out distribution, we calculate the amplitude, $G(k_1,k_2)$, by Monte Carlo sampling with typically 400-800 freeze-out phase-space coordinates selected according to (14) for each (k_1,k_2) pair. The freeze-out distributions for all resonance species is taken to be identical, and all T_r are set to 0.13 GeV to reduce the number of free parameters. To compare with data on the transverse projected correlation function[15], $\langle C(q_\perp)\rangle$, we must compute

$$\langle C(q_\perp)\rangle = 1 + \lambda\frac{\int d^3k_1 d^3k_2 \Theta(q_\perp;k_1,k_2)|G(k_1,k_2)|^2}{\int d^3k_1 d^3k_2 \Theta(q_\perp;k_1,k_2)G(k_1,k_1)G(k_2,k_2)} \ , \tag{16}$$

where the experimental constraints are built into Θ. For the present data Θ is non-vanishing only if $|k_{1\perp} - k_{2\perp}|$ is within 5 MeV/c of $q_\perp\pm$, $|k_{1z} - k_{2z}| \leq 0.1$ GeV/c, and if both y_1 and y_2 are in a certain interval $[y_{min}, y_{max}]$. The six dimensional integrals are computed by importance sampling using a model single inclusive distribution to generate typically ~ 200 pairs and repeating 2000-4000 times to insure convergence.

A good test of the numerical method is provided by reproducing the fitted curves in Ref.[15], which follow assuming the ideal inside-outside cascade distribution (15). In Fig 1a and 1d, we show that our calculations employing the reported parameters[15], $\tau_f = 6.4$ fm/c, $R_\perp = 7.3$ fm and $\lambda = 0.84$ for π^- in the rapidity interval $2 < y < 3$ and $\tau_f = 2.5$ fm/c, $R_\perp = 4.0$ fm, and $\lambda = 0.30$ in the interval $1 < y < 2$, do in fact provide a good fit to the data (note that the data have been corrected for Coulomb final state interactions).

Next, we show in Figs 1b,1e, the calculated curves for the case of non-ideal hadron resonance dynamics. For these calculations we chose $\Delta\eta = 0.8$ and considered $\tau_f =$

$R_\perp = 2, 4, 6$ fm. We have performed an additional Monte Carlo hadronic cascade calculation taking as input the output of the LUND fragmentation model[22] and found that with a $\sigma = 20$ mb, the true freeze-out distribution is roughly characterized by $\tau_f \sim R_\perp \sim 4$ fm for this reaction. In both Fig. 1b and 1e, the chaoticity parameter is fixed to $\lambda = 1$ as appropriate for completely chaotic sources. It is clear that the present data are consistent with the freeze-out distribution expected on the basis of a resonance gas model for the nuclear dynamics.

Next, in Figs. 1c,1f we show the remarkable result that the quark-gluon plasma freeze-out distribution is also consistent with the data. The reason is that the long lifetime of the plasma source leads to the same effect in this case as the inclusion of long lived hadronic resonances in Figs. 1b,1e. Note that our results for the plasma model differ substantially from those reported in Ref.[18]. We attribute this discrepancy to an improved numerical treatment and a more accurate definition of the experimental projected correlation function in the present work.

While it would be difficult to justify ruling out any of the three models from the present data, the "exotic" parameters obtained with the ideal inside-outside cascade model[12] are the least compelling, since it would be truly remarkable if the degree of coherence in such violent nuclear collisions were not negligible. Note that in Fig 1d, ideal dynamics with $\lambda = 1$ in fact fails to reproduce the data.

It has been suggested[11, 18] that the projected correlation function in terms of "outward" and "sideward" transverse momenta,

$$q_{out} = |\mathbf{q}_\perp \cdot \mathbf{K}_\perp|/K_\perp \ , \ q_{sid} = |\mathbf{q}_\perp - \mathbf{q}_{out}| \ , \tag{17}$$

could differentiate between hadronic and plasma models and provide an "unambiguous" signature of quark-gluon plasma formation. In Fig. 2a and 2b, we compare resonance gas and plasma model predictions for these projected correlation functions for the case $y_1 = y_2 = y^* = 2.5$. Indeed, quantitative differences can be seen. However, when integrated over a broad rapidity interval, $2 < y_\pi < 3$, as in the present data, most of those differences are washed out as can be seen in Figs. 2c,d. This shows that much higher statistics data will be required[31] to differentiate between present models[26] for nuclear collisions. Of course, additional experimental information will be essential to constrain further the dynamical degrees of freedom in both types of models. Especially important will be an independent direct measurement of resonance abundances[28], since in our hadronic scenario ω production is the main cause of the apparent long lifetime and radius.

3 Kaon Interferometry

To test whether kaon interferometry could be a more sensitive tool than pion interferometry, we apply the formalism discussed in the previous section to identical kaons, we obtain the result shown in Fig. 3. There, the arrows indicate the "pure" correlation function, i.e., those for which Coulombian corrections in the final state were not taken into account (see Ref.[5] for a discussion on Gamow correction factors). In Fig. 3.a and 3.c we show our results, employing the reported parameters of Ref[19],

respectively for the case of pions as well as for kaons. We see that, due to the absence of the ω's contribution to kaons, a substantial difference between the two dynamical scenarios arises. On Fig. 3.b and 3.d, we show the calculated curves corresponding to the plasma model [18] parameters. In this case, since resonances are not taken into account, practically no difference is observed for pions' and for kaon's correlation functions, when the Gamow factor is taken as unity. Therefore, kaon interferometry can clearly distinguish between our resonance gas scenario from the plasma one.

We should note, however, that when Coulombic final state interactions are taken into account, a dramatic suppression of the correlation function for small values of $q_\perp$ can be seen. This effect is even more significative for kaons, due to the increase in the mass factor. So, it seems that the Gamow factor practically kills the visibility of the effects because it affects the part of $C(k_1, k_2)$ where the Bose-Einstein enhancement is most significant. However, as already demonstrated by the NA35 Collaboration[15], it is possible (and desirable) to "ungamow" the interferometric results to exhibit more clearly this bosonic enhancement. If this is properly taken into account, we conclude that kaon-kaon interferometry is an useful tool for deciding whether the space-time geometry is determined mostly by long lived resonances or the slowness of the hadronization transition from a plasma state.

References

[1] G. Goldhaber, et al., Phys. Rev. 120 (1960) 300.

[2] G. I. Kopylov, Phys. Lett. 50B (1974) 572.

[3] E.V. Shuryak, Phys. Lett. 44B (1973) 387.

[4] F. B. Yano, S.E. Koonin, Phys. Lett. 78B (1978) 556.

[5] M. Gyulassy, S. K. Kauffmann, L. W. Wilson, Phys. Rev. C20 (1979) 2267.

[6] M. Gyulassy, Phys. Rev. Lett. 48 (1982) 454.

[7] S. Pratt, Phys. Rev. Lett. 53 (1984) 1219.

[8] D. Beavis, et al., Phys. Rev. C27 (1983) 910.

[9] W. A. Zajc, et al., Phys. Rev. C29 (1984) 2173.

[10] T. J. Humanic, Phys. Rev. C34 (1986) 191.

[11] S. Pratt, Phys. Rev. D33 (1986) 1314.

[12] K. Kolehmainen, M. Gyulassy, Phys. Lett. 180B (1986) 203.

[13] S. Pratt, Phys. Rev. D33 (1986) 72.

[14] Y. Hama, S. S. Padula, Proceedings of the 2nd International Workshop on Local Equilibrium in Strong Interaction Physics – LESIP II (1986), p. 63, ed. por P. Carruthers e D. Strottman; Y. Hama, S. S. Padula, Phys. Rev. D37 (1988) 3237.

[15] T. J. Humanic, et al. , Z. Phys. C38 (1988) 79; A. Bamberger, et al. Phys. Lett. B203 (1988) 320.

[16] M. G. Bowler, Z. Phys. C39 (1988) 81.

[17] A. N. Makhlin, Yu. M. Sinyukov, Z. Phys. C39 (1988) 69.

[18] G. Bertsch, M. Gong, M. Tohyama, Phys. Rev. C37 (1988) 1896.

[19] S. S. Padula and M.Gyulassy, LBL-26076 (1988) preprint, to be published in the Proceedings of Quark Matter'88, Nucl. Phys. A, ed. G.A. Baym, P. Braun-Munzinger and S. Nagamiya; M. Gyulassy, S. S. Padula, Phys. Lett. 217B (1989) 181.

[20] W. A. Zajc, Nevis Preprint R1384 (1987), to appear in Hadronic Multiparticle Production, World Scientific Press, P. Carruthers, ed. (1988).

[21] S. S. Padula, M. Gyulassy, S. Gavin, LBL-24674 (1988) preprint, to appear in Nucl. Phys. B.

[22] B. Andersson, et al., Nucl. Phys. B281 (1987) 289;
M. Gyulassy, CERN-TH.4794 (1987), Proc. Eight Balaton Conf. on Nucl. Phys. (ed. Z. Fodor, KFKI, Budapest 1987).

[23] J.D. Bjorken, Phys. Rev. D27 (1983) 140.

[24] E. A. Remler et al., Ann. Phys. 91 (1975) 295, 95 (1975) 455, 136 (1981) 293.

[25] M. Gyulassy, K. Frankel, and E. Remler, Nucl. Phys. A402 (1983) 596.

[26] Quark Matter '87, eds. R. Stock, H. Specht, and H. Satz, Z. Phys. C38 (1988) 117; Quark Matter '88, eds. G. Baym, P. Braun-Maunzinger, S. Nagamiya, Nucl. Phys. A (in press).

[27] G. Bertsch, M. Gong, L. McLerran, V. Ruuskanen, and E. Sarkkinen, Phys. Rev. D37 (1988) 1202.

[28] T. Müller, Proc. XIV Int. Symp. on Multiparticle Dynamics, eds. P.Yager, J.F. Gunion (World Scientific, Singapore, 1984), p. 528.

[29] P. Grassberger, Nucl. Phys. B120 (1987) 231.

[30] L. Van Hove, Z. Phys. C21 (1983) 93;
H. Gersdorff, et al, Phys. Rev. D34 (1986) 794.

[31] Y. Miake, et al., CERN/SPSC/88-37/SPSC/P239 (1988) report.

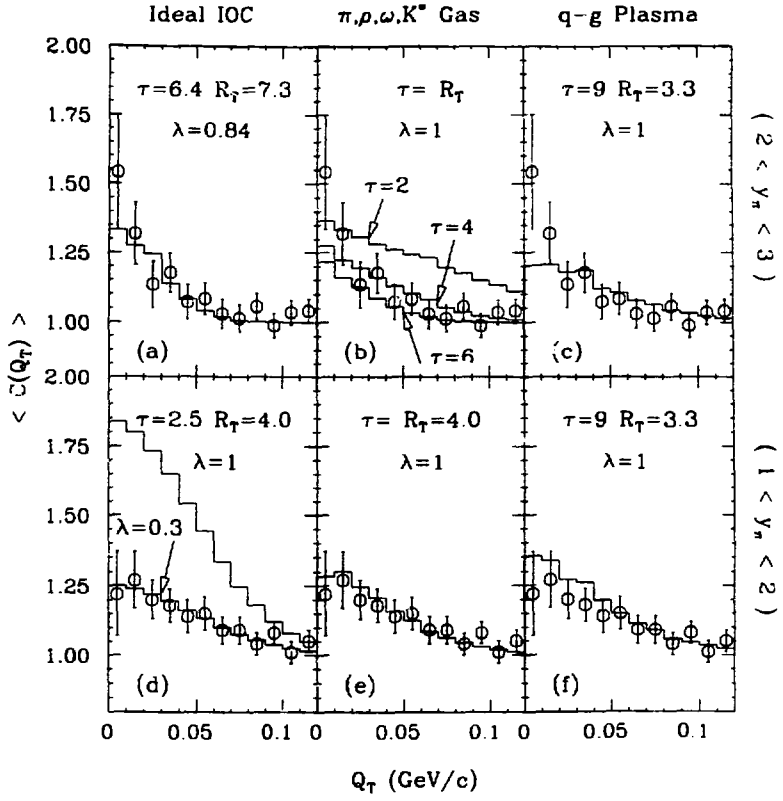

Figure 1:
Analysis of the transverse projected $\pi^-\pi^-$ correlation data of NA35[15]. The histograms in parts (a,d) are calculated assuming an ideal inside-outside cascade (IOC) source with parameters ($\tau \equiv \tau_f, R_T \equiv R_{\perp f}$) taken from [15]. In parts (b,e) a non-ideal resonance gas source is considered with parameters, $\tau \sim R_T \sim 4$ fm, as suggested by the ATTILA version of the LUND Fritiof model[22]. Parts (c,f) correspond to the quark-gluon plasma model of [18]. Parts (a-c) refer to the central rapidity region, $2 < y_\pi < 3$, and parts (d-f) refer to the region $1 < y_\pi < 2$.

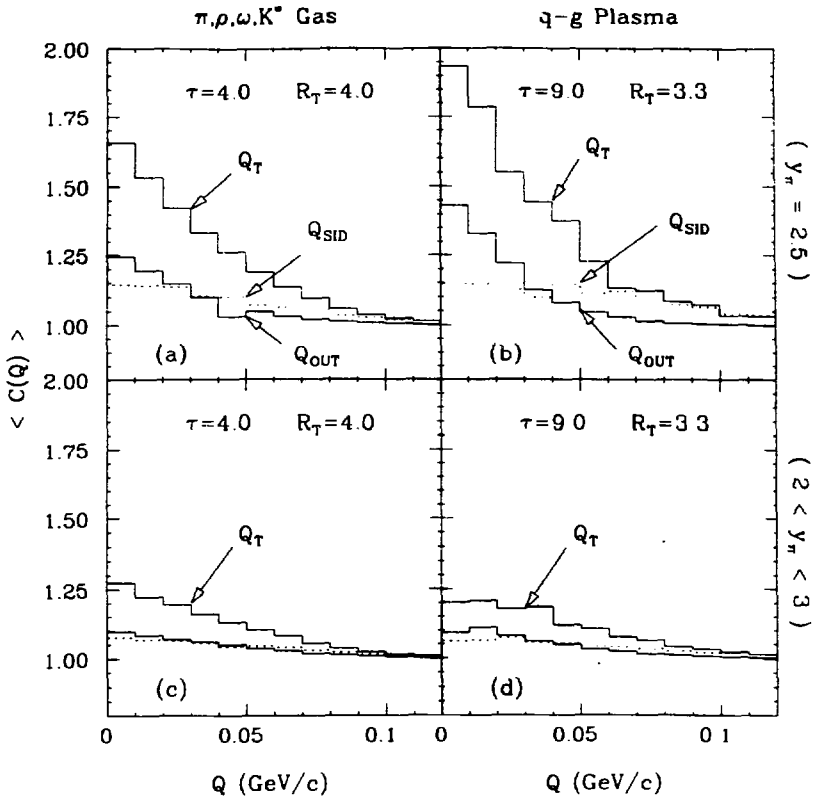

Figure 2:
Comparison of transverse projected "outward" and "sideward" interferometry calculated with a resonance gas model (a,c) and a quark-gluon plasma model (b,d). In (a,b) the two pion rapidities are restricted to $y_\pi = y^* = 2.5$, while in (c,d) a finite range, $2 < y_\pi < 3$, is considered. Q_T refers to the average transverse projected correlation function as in Fig. 1. The solid histograms labeled Q_{OUT} correspond to the projection of $\mathbf{q}_\perp$ parallel to $\mathbf{K}_\perp$ and the dashed histograms Q_{SID} to the projection of $\mathbf{q}_\perp$ perpendicular to $\mathbf{K}_\perp$.

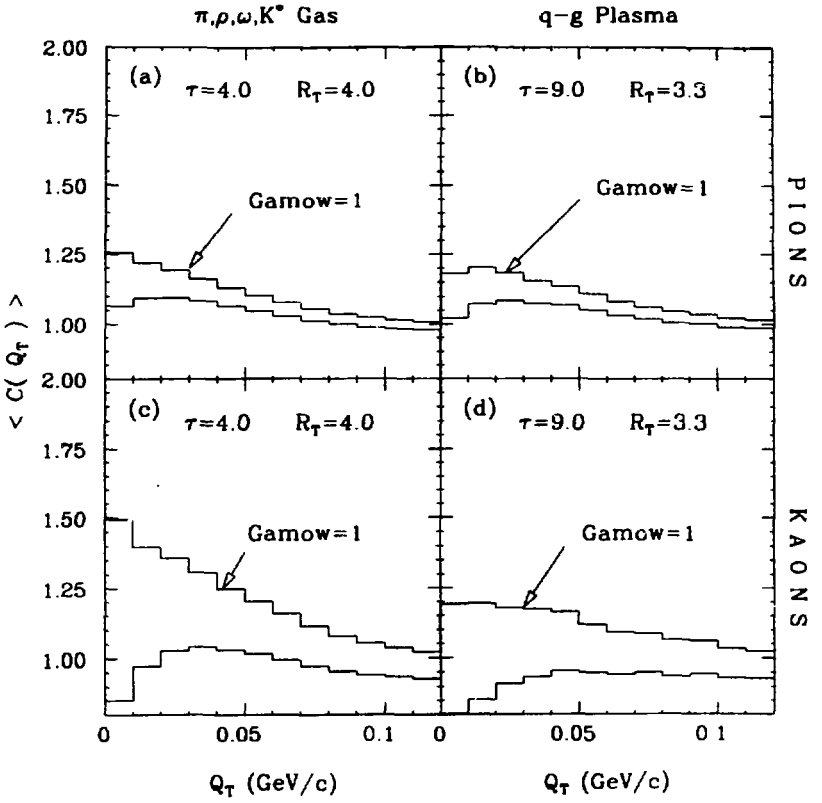

Figure 3:
Numerical results comparing pion and kaon correlation functions versus $q_\perp$, for $|\Delta y| < 1$, each particle being in the central rapidity region. The histograms not pointed by arrows correspond to the Gamow corrected results. We should emphasize that in all cases the chaoticity parameter is fixed to be unity.